



Control on Color Reflection Behavior

Xavier Granier, Cyrille Damez

► To cite this version:

Xavier Granier, Cyrille Damez. Control on Color Reflection Behavior. RR-5227, INRIA. 2004, pp.19.
inria-00070769

HAL Id: inria-00070769

<https://inria.hal.science/inria-00070769>

Submitted on 19 May 2006

HAL is a multi-disciplinary open access archive for the deposit and dissemination of scientific research documents, whether they are published or not. The documents may come from teaching and research institutions in France or abroad, or from public or private research centers.

L'archive ouverte pluridisciplinaire **HAL**, est destinée au dépôt et à la diffusion de documents scientifiques de niveau recherche, publiés ou non, émanant des établissements d'enseignement et de recherche français ou étrangers, des laboratoires publics ou privés.

Control on Color Reflection Behavior

Xavier Granier — Cyrille Damez

N° 5227

June 2004

Thème COG



*apport
de recherche*

Control on Color Reflection Behavior

Xavier Granier , Cyrille Damez *

Thème COG — Systèmes cognitifs

Projet IPARLA

Rapport de recherche n° 5227 June 2004 19 pages

Abstract: Nowadays, most of the computation of a rendering system is done in color space. Thus, the whole process, from acquisition (with a digital camera) and modelisation to display (on CRT/LCD displays) is color-based. Unfortunately, the reflection of a light on a surface is based on an approximation which can reduce the preservation of the color appearance. In this report, we present a new approach for color-based reflection that introduces a low overhead for an easy integration in current rendering systems. This approach allows also an easier control on the reflection behavior. In this report, we present also some possible applications, including global illumination, simple relighting and hardware rendering.

Key-words: Rendering, Illumination, Reflectance and Shading Models, Global Illumination, Relighting, Real-Time Rendering

* currently working at allegorithmic

Contrôle sur le Comportement de la Réflexion en Espace de Couleur

Résumé : Dans la grande majorité des systèmes de création d'images de synthèse, les calculs y sont effectués dans des espaces de couleur. Ainsi, tout le processus, de l'acquisition (avec par exemple un appareil photo numérique) et de la modélisation, vers l'affichage (comme sur des écrans CRT ou LCD), se déroule dans une même espace de travail, celui de la couleur. Cependant, cela entraîne une approximation dans le calcul de la réflexion d'une source de lumière sur une surface, réduisant notamment la possibilité de préserver l'apparence colorée d'un matériau. Dans ce rapport, nous présentons une nouvelle approche pour le calcul des réflexions dans un espace de couleur, approche qui n'introduit que de faibles changements dans le processus actuel, afin d'y faciliter son intégration. Elle permet aussi un certain contrôle sur le comportement de la réflexion. Enfin, nous présentons aussi les possibilités d'application pour cette méthode, comme le calcul de solution d'éclairage global, du ré-éclairage, ou du rendu sur carte graphique.

Mots-clés : Rendu, Éclairage, Propriétés de Réflexion, Éclairage Global, Ré-éclairage, Rendu Temps-Réel

1 Introduction

1.1 Motivation

Many solutions have been introduced to compensate for the restrictions of the current trichromatic color-based reflection model: new color basis [Pee91], color transformations [FDF94, DF00, DF02, WEV02], spectral estimation from color [Gla89, SFD99, Smi99]. The most accurate solution is to process the full rendering pipeline with a spectral representation of light [RF91, IP00, ZCB98]. But implementing these solutions requires large modifications in the current rendering process. They can also change the reflection behavior under standard color illuminants, and they do not allow an easy control on reflection behavior.

The approach presented in this report aims at using a single color representation during the whole rendering process. This prevents un-needed transformations, and introduces only a small change in current rendering systems. Our main assumption is that the input data of most rendering softwares will still be color-based (images from cameras, scanners, etc.), as will be the output devices (considering LCD/CRT displays). Therefore, we'll perform all of our computations in the input devices color space. Moreover, it is desirable to be coherent with the reflection model currently used in renderers: surfaces should keep the same aspect when lit by *white* colored illuminants (i.e., whose color is (k, k, k) with $k \neq 0$). Under this condition, users can keep the same approach to design light sources and surface properties, and they have the guaranty of a similar behavior under standard color illuminant. With this condition, we want also to provide a smooth transition between the classical approach and our new one, in order to provide and easy control on the reflection behavior.

From a developer point of view, we want to introduce only minimal changes to existing rendering systems. Therefore, the operator describing the interaction of light and surface reflectances has to be commutative.

Therefore, with this model, we do not try to bring the richness of a full spectral rendering, as spectral data is generally not provided for the description of surfaces reflectance, but a reflection model that better preserves appearance. In particular, we want to prevent the un-wanted color disappearance that can occur with the reflection model currently used, e.g. in the extreme case of a green surface reflecting a red light.

1.2 Color spaces

As defined in [SBS99], the color flow of a digital image can be divided into four spaces (cf Figure 1). The first one is the Sensor Space, from which an image or color characteristics are acquired. The last one is the Output Space. It contains also specific color spaces, that depends on the output device (RGB for display, CMY or CMYK for printers) and on the device constructor.

In between, we can define the Unrendered and the Rendered Space. In the Unrendered Space, the color is usually neither quantized nor tone-mapped and thus can be easily transformed. This

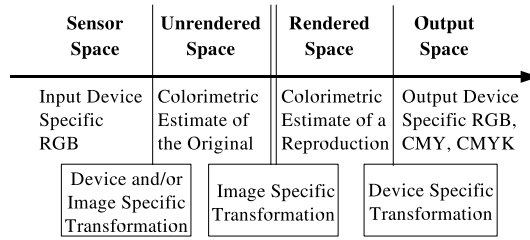


Figure 1: Digital Image Color Flow [SBS99]

space is used in current rendering systems and, in general, cannot be directly visualized. In the Rendered Space, the colors have lost their high-dynamic range information. Its purpose is to create a representation as close as possible to the one used by the output device. In this report, we will consider only the Unrendered Space, that is, the reflection space.

2 Previous work

Most rendering systems are currently using an RGB color space as their Unrendered Space, since the input data -acquired by a camera or any other imaging device, or defined by a user- usually provides RGB color information, and since the visualization output is in general an RGB display. Keeping the computation in this color space prevents to perform color space conversions.

Unfortunately, the current approach for the evaluation of light reflections on a surface is only achieved through a component by component multiplication. This fast scalar reflection is true only for a constant illuminant, and for colors defined by normalized color matching functions, as shown in [Bor91]. As a result, some color information can be lost. For example, a blue wall can appear black under a yellow illuminant. This becomes more visible in global illumination algorithms because they take into account the multiple reflections of the light.

This issue is due to the fact that the color matching functions are overlapping and that they are not orthogonal. With the "Spectral Sharpening" approach [FDF94, DF00, DF02], it is possible to find the "sharpest" functions obtained by a linear combination of the original color matching functions. For this sharp basis, the component by component multiplication for the reflection is valid for a larger range of colors.

A commonly chosen solution to improve the reflection behavior, is to use an appropriate spectral representation of lights and surface materials. Typically, a fine sampling of the spectral distribution is used. With their error-bound approach, Zeghers et al. [ZCB98] have shown that, in a diffuse environment, a global illumination solution without any visual difference can be generated with only four well selected spectral samples. Such spectral approaches manage to provide very precise results, by simulating effects like color dispersion, reflections and interferences through a layered material

[SFD99, IA00, HKY⁺00, HKY⁺01] at the price of a higher computational cost. In order to reduce the requirements in memory and computation, Iehl et al. [IP00] have developed a hierarchical model. They use an adaptive hierarchical representation for the spectral distribution. The appropriate hierarchical level to perform a given computation is chosen based on perceptual metrics. Raso et al. [RF91] have presented a piecewise polynomial approximation. Peercy [Pee91] has introduced a generalized linear approach, and proved that in general, three bases are sufficient for image synthesis purposes. Still, these methods can be costly compared to the standard reflection model, when they require a large number of spectral samples, and they need to have spectral input.

Thus, the main issue with spectral rendering is the availability of the input data. In general, and in our context, only a trichromatic color description is provided. Several approaches have been introduced to retrieve a spectral distribution from colors. The idea is to find a good spectral representation for a metamer (family of spectrum that are projected to the same color). The three lowest Fourier functions [Gla89] and exponential functions [SFD99] have been proposed since their variations are similar to the ones of color matching functions. With this approach, the retrieved spectra can have negative parts. In order to have only positive coefficients, Smits [Smi99] has introduced an approach based on linear combinations of the spectral distribution that represent 7 basic metamers (white, cyan, magenta, yellow, red, green, blue). These approaches are the closest related to our goal. Unfortunately, they do not guaranty a coherent behavior with the current rendering scheme, under generally used color illuminants.

Some recent work on shaders [Sta99, SFDC00] and on BRDFs [GH03] have shown that complex reflections can be obtained without a fine discretization. Peercy [Pee91] has shown that only three components are sufficient in the general case. Thus, we believe that a color reflection approach will still be the most suitable solution for image synthesis, if we can control the behavior of color reflection. Our goal is to provide a general approach that keeps the color definition of all material properties unchanged, but that will better preserve the color information under non-standard color illuminants.

The paper is organized as follows: we first present the bilinear model for reflections. We then introduce the corresponding new color operators, and how to estimate the required coefficients. We then present a tool to control the reflection behavior. This tool allows a smooth transition between regular reflection model and the one developed here. We also give some applications and their results, before we conclude and give directions to future work.

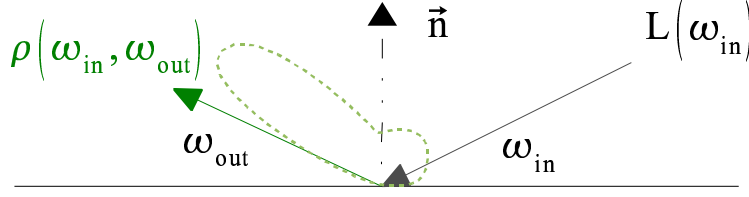


Figure 2: Geometric configuration of a reflection.

3 The bilinear model

The transformation from a spectral distribution $S(\lambda)$ to a trichromatic color representation¹ $[S_c]_{c \in \{r,g,b\}}$ is controlled by the color matching functions $\bar{B} = \{\bar{b}_c(\lambda), c \in \{r,g,b\}\}$:

$$\begin{bmatrix} S_r \\ S_g \\ S_b \end{bmatrix} = \begin{bmatrix} \langle \bar{b}_r, S \rangle \\ \langle \bar{b}_g, S \rangle \\ \langle \bar{b}_b, S \rangle \end{bmatrix},$$

where $\langle f, g \rangle = \int f \cdot g$ is the usual dot product for function spaces.

If the corresponding spectral basis $B = \{b_c(\lambda), c \in \{r,g,b\}\}$ exists, we can now express a spectral representative of a metamer for the light L and the BRDF ρ :

$$\begin{aligned} \tilde{L}(\lambda, \omega_{in}) &= \sum_{c \in \{r,g,b\}} L_c(\omega_{in}) b_c(\lambda) \\ \tilde{\rho}(\lambda, \omega_{in}, \omega_{out}) &= \sum_{c \in \{r,g,b\}} \rho_c(\omega_{in}, \omega_{out}) b_c(\lambda) \end{aligned} \quad (1)$$

with the notations in Figure 2.

Using these representatives, the appearance of this surface for a viewing direction ω_{out} is then defined by

$$\tilde{S}(\lambda) = \tilde{L}(\lambda, \omega_{in}) \tilde{\rho}(\lambda, \omega_{in}, \omega_{out}) \cos(\omega_{in}),$$

and the corresponding color is

$$\tilde{C} = \begin{bmatrix} \langle \tilde{S}, \bar{b}_r \rangle \\ \langle \tilde{S}, \bar{b}_g \rangle \\ \langle \tilde{S}, \bar{b}_b \rangle \end{bmatrix}. \quad (2)$$

By combining Equation 2 and Equation 1, we obtain a bilinear solution, similar to [Zmu92]: $\forall c \in \{r,g,b\}$

$$\tilde{C}_c = \cos(\omega_{in}) \sum_{d \in \{r,g,b\}} \sum_{e \in \{r,g,b\}} L_d(\omega_{in}) \rho_e(\omega_{in}, \omega_{out}) k_{d,e}^c, \quad (3)$$

¹We will use RGB in this document but our approach can be applied to similar color spaces like XYZ.

where the 27 coefficients $k_{d,e}^c$ are unique for a given spectral basis and a given set of color matching functions:

$$k_{d,e}^c = \langle b_d b_e, \bar{b}_c \rangle. \quad (4)$$

In fact, the number of coefficients reduces to 18, due to the symmetry in the construction:

$$k_{d,e}^c = k_{e,d}^c. \quad (5)$$

For the rest of the document, we note them as 3 matrices:

$$\mathbf{K}_e = \begin{bmatrix} k_{e,r}^r & k_{e,g}^r & k_{e,b}^r \\ k_{e,r}^g & k_{e,g}^g & k_{e,b}^g \\ k_{e,r}^b & k_{e,g}^b & k_{e,b}^b \end{bmatrix}, \quad e \in \{r, g, b\}.$$

With this notation, the Equation 3 defines a new reflection model that can be simplified into a matrix multiplication:

$$\tilde{C} = \cos(\omega_{in}) \mathbf{R}(\omega_{in}, \omega_{out}) [L_c(\omega_{in})]_{c \in \{r, g, b\}}, \quad (6)$$

where the matrix $\mathbf{R}(\omega_{in}, \omega_{out})$ is defined as

$$\mathbf{R}(\omega_{in}, \omega_{out}) = \sum_{e \in \{r, g, b\}} \rho_e(\omega_{in}, \omega_{out}) \mathbf{K}_e. \quad (7)$$

4 New reflection operators

In order to introduce only a small change in current rendering systems, we define new multiplication and division operators on colors, and use them to express the new reflection approach.

4.1 New color-space operators

The advantage of the model defined in the Equation 6 is that the reflectance property and the light can still commute, thanks to the symmetry property of the coefficients $k_{d,e}^c$. We can then redefine the multiplication on colors (denoted by \otimes) as

$$C = C^1 \otimes C^2 = \left[\sum_{e \in \{r, g, b\}} C_e^1 \mathbf{K}_e \right] C^2 = C^2 \otimes C^1.$$

Moreover, provided that the corresponding matrix is not singular, a division operator on colors (denoted by \oslash) can also be introduced:

$$C^2 = C \oslash C^1 = \left[\sum_{e \in \{r, g, b\}} C_e^1 \mathbf{K}_e \right]^{-1} C.$$

This operator is not defined for colors that satisfy the condition

$$\det \left[\sum_{e \in \{r,g,b\}} C_e \mathbf{K}_e \right] = 0.$$

This is a third degree polynomial equation with C_r , C_g and C_b as unknowns, whose coefficients and solutions depend on the color basis used, and which define a curved surface in color space. However, we may note that when all three \mathbf{K}_e matrices are non-singular, purely red, green or blue colors can be divided by, which isn't the case when using the classical component-by-component color multiplication.² We will further discuss this issue in the particular case of the ISO RGB color base in Section 5.3.

4.2 New color reflection model

With these new operators, we can then rewrite the Equation 6 as

$$\tilde{C} = \begin{bmatrix} \rho_r(\omega_{in}, \omega_{out}) \\ \rho_g(\omega_{in}, \omega_{out}) \\ \rho_b(\omega_{in}, \omega_{out}) \end{bmatrix} \otimes \begin{bmatrix} L_r(\omega_{in}) \cos(\omega_{in}) \\ L_g(\omega_{in}) \cos(\omega_{in}) \\ L_b(\omega_{in}) \cos(\omega_{in}) \end{bmatrix}. \quad (8)$$

The reflection computation is still a three step process:

1. Evaluation of the reflectance (i.e., the BRDF) $[\rho_c(\omega_{in}, \omega_{out})]_{c \in \{r,g,b\}}$
2. Evaluation of the incident light $[L_c(\omega_{in}) \cos(\omega_{in})]_{c \in \{r,g,b\}}$
3. Reflection with the Equation 8.

To implement this reflection model in an existing rendering system, only the color multiplication operator has to be rewritten.

Note that, for complex shading, most of the time is spent in the two first steps: the computation of the reflectance color or in the evaluation of the incident light (like in global illumination algorithms). Our approach requires to modify only on the final operation (the multiplication of incoming light with the reflectance color).

4.3 Possible Simplifications

This process can be simplified in most cases. For the diffuse materials, the matrix \mathbf{R} (see the Equation 7) is now direction-independent. It can be then evaluated once and stored as the material description.

²This classical approach corresponds to three singular matrices, whose coefficients $k_{e,c}^c$ are 1, and 0 elsewhere.

Moreover, it is often the case that the BRDF directional properties are independent of the color component, that is,

$$\begin{bmatrix} \rho_r(\omega_{in}, \omega_{out}) \\ \rho_g(\omega_{in}, \omega_{out}) \\ \rho_b(\omega_{in}, \omega_{out}) \end{bmatrix} = \rho(\omega_{in}, \omega_{out}) \begin{bmatrix} \rho_r \\ \rho_g \\ \rho_b \end{bmatrix}.$$

In such cases (e.g. Phong's specular lobe) a direction-independent matrix \mathbf{R} can also be pre-computed, based on the reflection coefficients $[\rho_c]_{c \in \{r,g,b\}}$. Then the Equation 6 can be simplified to

$$\tilde{\mathbf{C}} = (\cos(\omega_{in})\rho(\omega_{in}, \omega_{out}))\mathbf{R} \begin{bmatrix} L_r(\omega_{in}) \\ L_g(\omega_{in}) \\ L_b(\omega_{in}) \end{bmatrix}.$$

The coefficients $k_{d,e}^c$ give us an easy way to convert the color representation of a BRDF, and to extend the reflection model to matrix approaches.

5 Estimation of the coefficients $k_{d,e}^c$

As said in the introduction, we want to keep a coherent behavior with the standard reflection model. Thus, we first introduce a coherent behavior condition that allows our approach to match the required reflection behavior for a *white* light source.

Even if with this new condition, there is not enough condition to completely determine the coefficient values. We show then how we can Estimate them from a set of color matching functions, defined by a regular spectral sampling. This first approximation is then minimized to fit this new condition.

5.1 Coherent behavior condition

As previously stated, when the color matching functions are normalized, the standard reflection model do not show any artefacts, as show in [Bor91]. For a user point of view, this means that a color is equal to the color of the surface reflectance under a *white* light. When the color space is not normalized, we still want to keep this property to be coherent with the current model, in order to ease the design of material properties. Then, the reflectance multiply by a white light has to be the reflectance scaled by the light intensity. This leads to the equation (where \mathbf{I} is the identity matrix):

$$\mathbf{K}_r + \mathbf{K}_g + \mathbf{K}_b = \mathbf{I}. \quad (9)$$

5.2 Estimation from color matching functions

For this evaluation, we can express an approximated version of the color matching functions by:

$$\forall c \in \{r, g, b\}, \bar{b}_c(\lambda) \simeq \sum_{j=1}^n \bar{\tau}_j \phi_j(\lambda) \quad (10)$$

where $(\bar{\tau}_i, i \in [1..n], c \in \{r, g, b\})$ are the regular sampled values of the matching functions, and $(\phi_i(\lambda), i \in [1..n])$ is an interpolation basis.

If we want the projection into the color basis to be orthogonal, the color basis has to be a linear combination of the color matching functions, that is:

$$\begin{bmatrix} b_r \\ b_g \\ b_b \end{bmatrix} = \mathbf{M} \begin{bmatrix} \bar{b}_r \\ \bar{b}_g \\ \bar{b}_b \end{bmatrix}. \quad (11)$$

Note that, since the projection is orthogonal, the representatives defined in the Equation 1 minimize the distance to all the spectral distributions of the metamer.

As these two basis are duals, i.e. $\langle \bar{b}_i, b_j \rangle = \delta_{i,j}$,

$$\mathbf{M}^{-1} = \begin{bmatrix} \langle \bar{b}_r, \bar{b}_r \rangle & \langle \bar{b}_r, \bar{b}_g \rangle & \langle \bar{b}_r, \bar{b}_b \rangle \\ \langle \bar{b}_g, \bar{b}_r \rangle & \langle \bar{b}_g, \bar{b}_g \rangle & \langle \bar{b}_g, \bar{b}_b \rangle \\ \langle \bar{b}_b, \bar{b}_r \rangle & \langle \bar{b}_b, \bar{b}_g \rangle & \langle \bar{b}_b, \bar{b}_b \rangle \end{bmatrix}. \quad (12)$$

We have now the approximated expression of the color basis and its dual, and from them we can compute the coefficients $\tilde{k}_{d,e}^c$ using the Equation 4. They will be a first approximation of the final coefficients $k_{d,e}^c$. Note that, by construction, these coefficients follow the symmetry condition.

The coefficients can be slightly away from the coherent behavior condition, even for normalized color matching functions. Therefore, a minimization process under the this condition and the symmetry ones can adjust them to fit the needed conditions.

5.3 Estimation for the ISO RGB color space

For our purpose, we used the ISO RGB color space which is in the process of becoming a standard (see Figure 3 and [ISO21]). Since it is an Unrendered Color Space, there are no specified dynamic range or viewing conditions, making it suitable for lighting computations. Furthermore, the color matching functions are normalized, making the coherent behavior condition implicit.

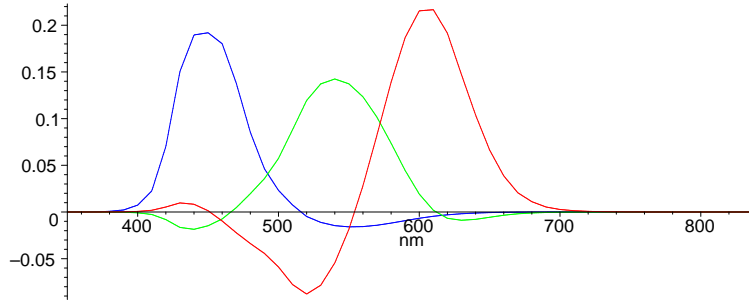


Figure 3: The ISO RGB color matching functions.

We present here, in a matrix notation, the coefficients obtained for the ISO RGB color space:

$$\begin{aligned}
 \mathbf{K}_r &= \begin{bmatrix} .6533043776 & .2708567778 & .0758388444 \\ .0594368555 & -.0413179278 & -.01811892773 \\ -.01119056664 & .0005536667 & .0106368999 \end{bmatrix} \\
 \mathbf{K}_g &= \begin{bmatrix} .2708567778 & -.2135258222 & -.05733095555 \\ -.0413179278 & .9943860889 & .0469318388 \\ .0005536667 & -.04014829995 & .0395946333 \end{bmatrix} \\
 \mathbf{K}_b &= \begin{bmatrix} .0758388444 & -.05733095555 & -.01850788891 \\ -.01811892773 & .0469318388 & -.02881291107 \\ .0106368999 & .0395946333 & .9497684667 \end{bmatrix}.
 \end{aligned}$$

Note that the determinant of the matrices $\mathbf{K}_r, \mathbf{K}_g$ and \mathbf{K}_b are non-zero. This does not ensure that the division is always possible, but as pointed out in Section 4.1, this case is restricted to a surface in color space. For quantized colors, such as the standard 8-bit color definition, it only occurs at $(0, 0, 0)$.

6 Introducing Control on the Reflection Behavior

6.1 Analysis of the Coefficient Meaning

The coefficients for the ISO RGB color matching functions, we can notice that the bigger ones are the $k_{i,i}^i$. For the classical reflection behavior, their value is 1, and the other coefficients are null, that correspond to the case where no transfer occur from a color component to an other one. In the ISO RGB case, most of the transfer occur to the red color component (see Section 7). This correspond also to the smallest $k_{i,i}^i$ value.

So intuitively, the $k_{i,i}^i$ coefficients correspond to the amount of energy that is not transferred from one color component i and reciprocally, $1 - k_{i,i}^i$ correspond to the amount of energy that is transferred to the color component i .

We can also notice that the coefficient which control the transfer to the component i are $k_{j,k}^i, \forall j \in \{r, g, b\} \forall k \in \{r, g, b\}$, as shown in the Equation 3. Only those have to be modified in order to change the reflection behavior component i .

6.2 User Modification of the Coefficients

One way to control the behavior of the reflection, is to select the amount of energy that will be transferred on a component: $\alpha_i, i \in \{r, g, b\}$. Based on the previous observations, we can simply modify the coefficients $k_{i,i}^i$ to become:

$$k_{i,i}^i = 1 - \alpha_i, \forall i \in \{r, g, b\}.$$

We can then adjust the rest of the coefficients $k_{d,e}^c$ the following way:

$$k_{j,k}^i = \beta_i k_{j,k}^i.$$

This modification preserve the symmetry condition (see the Equation 5) since

$$k_{j,k}^i = \beta_i k_{j,k}^i = \beta_i k_{k,j}^i = k_{k,j}^i.$$

The new coefficients have also to follow the Coherent Behavior Condition, as defined in the Equation 9. This leads to determine the values of β_i as:

$$\beta_i = \frac{\alpha_i}{1 - k_{i,i}^i}, \forall i \in \{r, g, b\}.$$

Note that, when $\alpha_i = 0$ (i.e., there is no transfer on the i th component), then $\beta_i = 0$

7 Applications and results

7.1 Global illumination

We have used our new approach to compute global illumination solutions. The two following scenarios will show the effect of our approach on direct lighting and indirect lighting.

For the direct lighting scenario, we have implemented a simple ray-tracing strategy. The $k_{d,e}^c$ coefficients are used to convert the color definition of surfaces into a matrix representation. For a

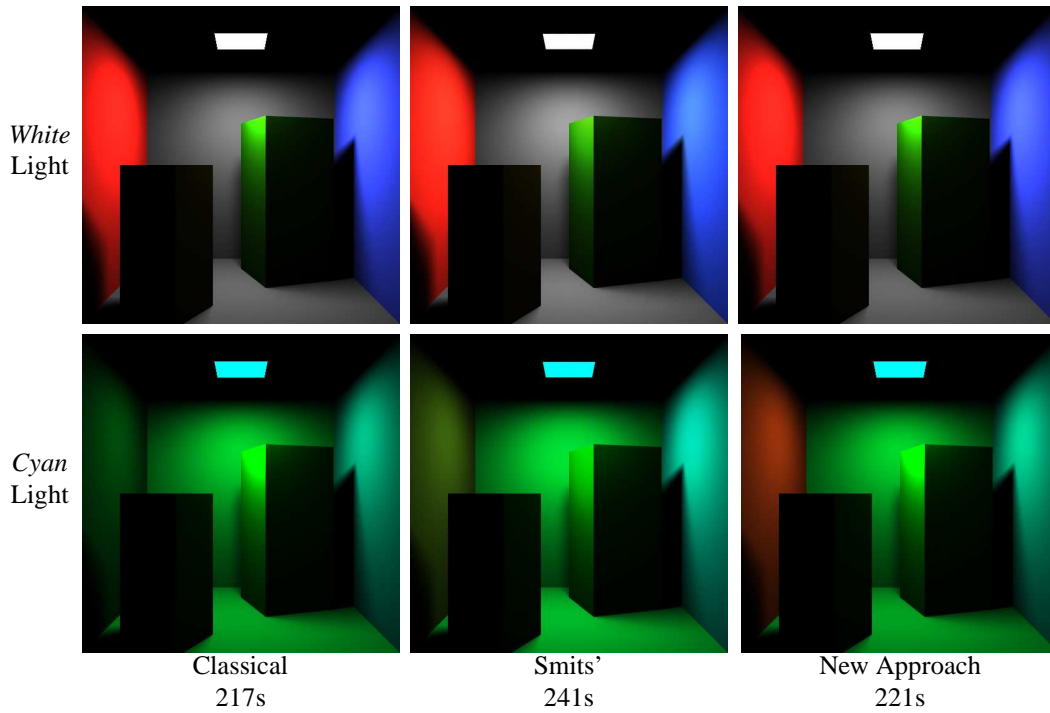


Figure 4: Direct lighting of a Cornell box.

comparison, we also implemented Smits' [Smi99] approach to convert the initial RGB data to a full spectral definition of materials. Figure 4 shows the results on a Cornell box, for the classical approach, the spectral one, and ours. Note that our new technique has only a small impact (2% more) on the rendering time ³. The more complex the shader, the smaller the relative impact on the performance, since our approach doesn't change the way reflectance are computed, but only the final multiplication between the incoming light and the estimated reflectance.

By construction, under a *white* illuminant, our approach provides the same solution as the classical model, whereas the spectral solution creates a larger red highlight. This is due to the coherent behavior condition (see Section 5.1). For the lighting under a *cyan* illuminant, our approach preserves the red aspect of the wall that completely disappears with the classical reflection.

Most of the loss in color may appear in indirect lighting. To demonstrate this effect, we designed a "psychedelic" lounge for which we computed a radiosity solution. Note that for the implementation of our approach, we had to rewrite only the multiplication operator for colors. In this scene, the light sources are facing the *blue* ceiling. The indirect light is therefore mostly blue. As shown in Figure 5,

³on an Intel Pentium4 2.6 GHz with 1 GB of memory



Figure 5: The "psychedelic" lounge illuminated. Note that the overall redness is better preserved in our approach. In the left painting, we have also better preserved the red color.

once again our approach preserves the color appearance whereas the classical approach creates a more grayish aspect. This is more noticeable on the walls and on the leftmost painting, for which the red color is less attenuated. The example of this painting shows that in a less colored environment, some visible differences can appear.



Figure 6: Adjusting the transfer. The left image is obtained using ISO RGB coefficients. The right one with a modification to allow more transfer to the blue.

We also computed a solution with a different set of coefficients (see Figure 6). For this one, we modify the ISO RGB coefficients as described in Section 6, in order to have a lot of transfer to the blue component: $(\alpha_r, \alpha_g, \alpha_b) = (0, 0, 1)$. We can notice that the resulting solution has a more blueish

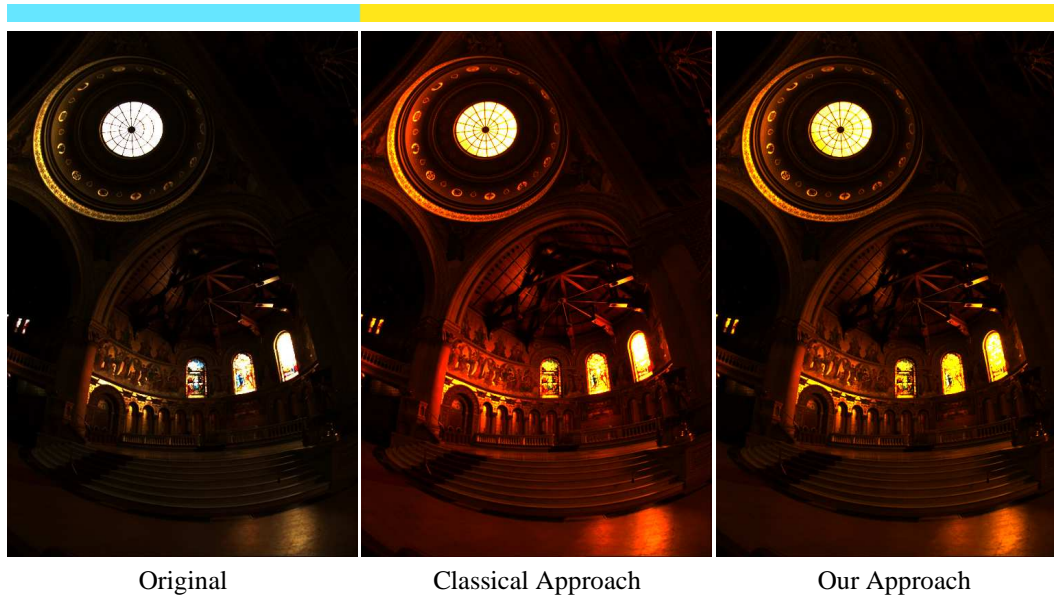


Figure 7: Changing outdoor light on the memorial. Note the over-saturated red in the classical approach.

aspect than the ISO RGB one, without modifying any material property. As the lighting is mostly indirect, it will be difficult to obtain the same behavior with an other approach.

7.2 Simple relighting

We also used our reflection model to implement a basic relighting approach, with a simple change on the color of the light source. Working on high-dynamic range images [DM97], the relighting process is simply the division of the pixel color by the previous illuminant and its multiplication with the new illuminant. We have experimented a change from a blue-sky light source (0.4 0.9 1.0) to a yellow illuminant (1.0 0.9 0.1). Visibly (see Figure 7), the color information is better preserved with our approach.

7.3 Hardware accelerated rendering

As the last application, we have implemented our approach using the current graphics hardware programmability⁴. For this purpose, we use the iridescent BRDF model [GH03], to show a component-

⁴ARB_{vertex/fragment}_program OpenGL extensions on an NVIDIA Quadro FX 500

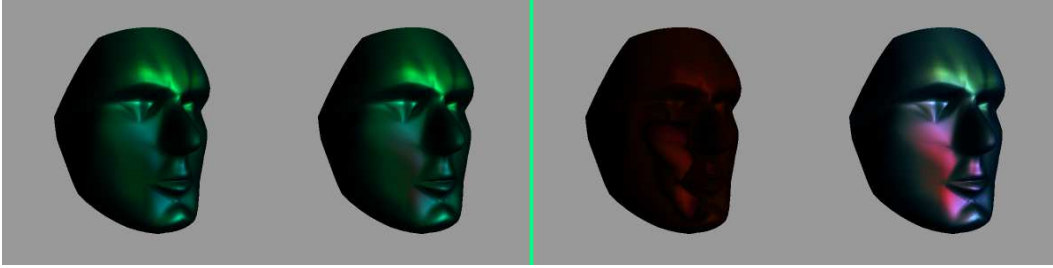


Figure 8: Hardware implementation: a) regular reflection – b) our approach – c) difference – d) reflection under a *white* light source. For a) and b), the color of the light source is shown in the middle rectangle. Note that the red highlight on the cheek (cf d)) has disappeared with the classical approach (cf a)) and it is still present with our approach.

dependent behavior. The classical solution to increase color preservation, is to represent a material property by a 3×3 matrix. Then for a component-dependent BRDF, 9 functions have to be defined. With our approach, we keep the 3-component color definition, and simply add 11 instructions at the end of the fragment program for the reflection evaluation. The original shader is composed of a fragment program with 42 instructions and a vertex program with 70 instructions. This has only a small impact on the framerate (160 fps instead of 170 fps for a 400×400 image).

The results are visible in Figure 8. Once again, the color appearance is better preserved. The red reflection is still present in our approach whereas it disappeared in the classical solution.

8 Conclusion

In this report, we have presented new multiplication and division operators adapted to the color representation, in order to have a better preservation of color appearance in reflections. This new approach requires a minimal change to be implemented in current rendering systems, and behaves coherently with respect to existing solutions. This coherent behavior allows users to keep the same approach when designing the appearance of surfaces.

We have also presented an approach to control the reflection behavior resulting from these operators. This is done by an adaptation of the original coefficients, adjusting the amount of energy that is transferred to a selected component.

As examples, we have implemented our solution in three possible applications: global illumination, simple relighting and hardware rendering. We have based our experiments on the upcoming new standard for RGB Unrendered Color Space, the ISO RGB, but our approach can be applied to other similar Unrendered Color Spaces. The results have shown a better behavior in preserving color information, with a low overhead in implementation and computation.

Future work

We believe that this work can be extended in two ways: coefficient computation and accuracy.

With our choice of the ISO RGB color space, the results have shown more transfer from the blue and green components to the red one. Even if our approach allows to adjust the coefficients in order to give more control on the reflection behavior, we still not have a complete control. In the near future, we want to develop a new coefficient computation that will give a complete control to the user.

For accuracy, using perceptual studies, we plan to investigate how the user expects the scene to appear under different lighting conditions. This calls for a comparison with the results obtained through classical color constancy approaches.

Acknowledgment

We want to acknowledge Wolfgang Heidrich, Torsten Möller, Christophe Schlick and Patrick Reuter for spending time in discussion on this topic, the REVES/INRIA-Sophia project for providing the GIS Global Illumination Software, and Paul Debevec for high-dynamic range images. Part of this project has been done during the post-doc of Xavier Granier at the University of British Columbia, under the PIMS post-doctoral fellowship.

References

- [Bor91] Carlos F. Borges. A Trichromatic Approximation Method for Surface Illumination. *Journal of Optical Society of America*, 8(8):1319–1323, August 1991.
- [DF00] Mark S. Drew and Graham D. Finlayson. Spectral Sharpening with Positivity. *Journal of Optical Society of America*, 17(8):1361–1370, 2000.
- [DF02] Mark S. Drew and Graham D. Finlayson. Multispectral Processing Without Spectra. Technical Report SFU-CMPT-TR2002-02, School Of Computing Science - Simon Fraser University, 2002.
- [DM97] Paul E. Debevec and Jitendra Malik. Recovering High Dynamic Range Radiance Maps from Photographs. In *Computer Graphics (SIGGRAPH 99 Proc.)*, Annual Conference Series, pages 369–378. ACM, August 1997.
- [FDF94] Graham D. Finlayson, Mark S. Drew, and Brian V. Funt. Spectral Sharpening: sensor transformations for improved constancy. *Journal of Optical Society of America*, 11(5):1553–1563, May 1994.
- [GH03] Xavier Granier and Wolfgang Heidrich. A Simple Layered RGB BRDF Model. *Graphical Models*, 65(4):169–257, July 2003.

- [Gla89] Andrew S. Glassner. How to derive a Spectrum From a RGB triplet. *IEEE Computer Graphics and Applications*, 9(4):95–99, July 1989.
- [HKY⁺00] H. Hirayama, K. Kaneda, H. Yamashita, , and Y. Monden. An Accurate Illumination Model for Objects Coated with Multilayer Films. In *Eurographics 2000 Short Presentations*, pages 145–150. Eurographics, september 2000.
- [HKY⁺01] H. Hirayama, K. Kaneda, H. Yamashita, Y. Yamaji, and Y. Monden. Visualization of optical phenomena caused by multilayer films based on wave optics. *The Visual Computer*, 17(2):106–120, March 2001.
- [IA00] Isabelle Icart and Didier Arques. A Physically-Based BRDF Model for Multilayer Systems with Uncorrelated Rough Boundaries. In *Eurographics Rendering Workshop 2000*, pages 353–364. Eurographics, June 2000.
- [IP00] Jean-Claude Iehl and Bernard Péroche. An adaptative spectral rendering with a perceptual control. *Computer Graphics Forum (Proceedings of Eurographics 2000)*, 19(3), 2000.
- [ISO21] Graphic Technology and Photography Colour target and procedures for the colour characterisation of digital still cameras (DSCs)., ISO 17321. draft document available at <http://www.cs.sfu.ca/~mark/ftp/IsoWg18/>.
- [Pee91] Mark S. Peercy. Linear Color Representaation for Full Spectral Rendering. In *Computer Graphics (SIGGRAPH 91 Proc.)*, Annual Conference Series, pages 191–198. ACM, 1991.
- [RF91] Maria Raso and Alain Fournier. A Piecewise Polynomial Approach to Shading Using Spectral Distribution. In *Proceedings of Graphics Interface 91*, pages 40–46. Canadian Human-Computer Communications Society, Morgan Kauffman, June 1991.
- [SBS99] Sabine Süsstrunk, Robert Buckley, and Steve Swen. Standard RGB Color Spaces. In *The Seventh Color Imaging Conference: Color Science, Systems, and Applications*, pages 127–134. IS&T - The Society for Imaging Science and Technology, November 1999.
- [SFD99] Yinlong Sun, F. David Fracchia, and Thomas W. Calvert Mark S. Drew. Deriving Spectra from Colors and Rendering Light Interference. *IEEE Computer Graphics and Applications*, 19(4):61–67, July 1999.
- [SFDC00] Yinlong Sun, David Fracchia, Mark Drew, and Thomas Calvert. Rendering Iridescent Colors of Optical Disks. In *Eurographics Rendering Workshop 2000*, pages 353–364. Eurographics, Eurographics, June 2000.
- [Smi99] Brian Smits. An RGB to Spectrum Conversion for Reflectances. *Journal of Graphics Tools*, 4(4):11–22, 1999.

- [Sta99] Jos Stam. Diffraction Shader. In *Proceedings of SIGGRAPH 99*, Computer Graphics Proceedings, Annual Conference Series, pages 75–84. SIGGRAPH, ACM Press, August 1999.
- [WEV02] Greg Ward and Elena Eydelberg-Vileshin. Perfect RGB Rendering Using Spectral Prefiltering and Sharp Color Primary. In *Rendering Techniques 2002 (Proceedings of the Thirteenth Eurographics Workshop on Rendering)*, pages 117–124. Eurographics, ACM Publisher, June 2002.
- [ZCB98] E. Zeghers, S. Carré, and Kadi Bouatouch. Error-Bound Wavelength Selection for Spectral Rendering. *The Visual Computer Journal*, 13(9-10):424–434, January 1998.
- [Zmu92] Michael D Zmura. Color constancy : surface color from changing illumination. *Journal of the Optical Society of America*, 9(3):490–493, March 1992.



Unité de recherche INRIA Futurs
Parc Club Orsay Université - ZAC des Vignes
4, rue Jacques Monod - 91893 ORSAY Cedex (France)

Unité de recherche INRIA Lorraine : LORIA, Technopôle de Nancy-Brabois - Campus scientifique
615, rue du Jardin Botanique - BP 101 - 54602 Villers-lès-Nancy Cedex (France)
Unité de recherche INRIA Rennes : IRISA, Campus universitaire de Beaulieu - 35042 Rennes Cedex (France)
Unité de recherche INRIA Rhône-Alpes : 655, avenue de l'Europe - 38334 Montbonnot Saint-Ismier (France)
Unité de recherche INRIA Rocquencourt : Domaine de Voluceau - Rocquencourt - BP 105 - 78153 Le Chesnay Cedex (France)
Unité de recherche INRIA Sophia Antipolis : 2004, route des Lucioles - BP 93 - 06902 Sophia Antipolis Cedex (France)

Éditeur
INRIA - Domaine de Voluceau - Rocquencourt, BP 105 - 78153 Le Chesnay Cedex (France)
<http://www.inria.fr>
ISSN 0249-6399